*Rev. Roum. Sci. Techn.– Électrotechn. et Énerg.*
Vol. **69**, *2*, pp. 141–146, Bucarest, 2024

# EFFICIENT DSP-BASED REAL-TIME IMPLEMENTATION OF ANFIS REGULATOR FOR SINGLE-PHASE POWER FACTOR CORRECTOR

SAMIA LATRECHE[1], AMAR BOUAFASSA[2], BADREDDINE BABES[3,*], OUALID AISSA[4]

**Keywords: Active power factor correction (A-PFC) converter; Adaptive neural-fuzzy inference system (AN-FIS); Predictive current controller; dSPACE card 1104.**

**As a widely used technology, active power factor corrector (A-PFC) circuits face many control challenges, such as nonlinearity and uncertainties. With more and more power electrical appliances that are connected to the utility grid, the A-PFC is for the task of improving the power quality (PQ) to meet the requirement of the international standards, and this results in great challenges for keeping the total harmonic distortion (THD) as long as a power factor in the desired ranges. To this end, this paper focuses on the simulation and real-time implementation of a combined adaptive neural-fuzzy inference system (ANFIS) and predictive current controller for a single-phase PFC rectifier. The proposed control method has a simple, low-cost structure for better response and robustness. The performance of the proposed control approach was evaluated in real-time based on the dSPACE 1104 digital signal processor for different reference and load conditions. The results obtained from simulation and experimental tests validate the superiority of the proposed approach by evidencing a unity power factor, lower THD, fast dynamic response, and robustness against fast load and output voltage variations.**

## 1. **INTRODUCTION**

With the rapidly increasing use of power electronic equipment and injection of a huge number of current harmonics into the distribution networks, the requirements imposed by international standards and grid codes to their operation as front ends for both distributed energy resources and loads have increased [1,2]. Indeed, switched-mode power supplies (SMPS) with power factor correction (PFC) techniques are mandatory for various industrial applications such as welding, chargers for electric vehicles, DC motor drives, and LED lights. Therefore, the PFC circuits are becoming imperative on SMPS as more stringent PQ regulations and strict limits on the total harmonic distortion of input current are imposed, such as IEC 61000-3-2 and IEEE 519 [3]. Most active PFC circuits and SMPS involve two stages: *i*) a front-end bridge rectifier and *ii*) a dc-dc converter based on the output voltage requirement such as boost, buck-boost, SEPIC, and Cuk. PFC boost converters at the front end are required where the preferred output voltage is high. Boost-type circuits are widely employed in commercial power supplies because of their low cost, high efficiency, power factor, and control simplicity (Fig. 1) [4]. One of the major issues in PFC circuits is the development of a suitable controller that should be robust to parametric variations, load disturbance, and input voltage variations. Literature regarding active power factor correction has introduced many modern control theories focused on achieving high performance against various uncertainties and parameter variations. These control methods were employed to control the output voltage of the ac-dc rectifier, including sliding mode control [4–6], fuzzy logic [7,8], fractional control [9], and artificial intelligent control [10]. Artificial intelligence control techniques like fuzzy logic (FL) and artificial neural networks (ANN) have been intensively applied in industrial applications because they are not limited by mathematical assumptions used in control theories. A fuzzy logic controller (FLC) is widely used to control complex systems with uncertainty parameters; it does not need a full understanding of the mathematical background and nature of the complicated mechanisms of the studied system. However, the fuzzy system needs the knowledge of an expert, which is usually expressed in linguistic terms and by accurate membership functions (MFs). For these reasons, artificial neural networks based on learning ability can compensate for this lack and enhance the performance of fuzzy logic. By fusing the human-like thinking capability of the fuzzy inference system and the learning ability of the artificial neural network, an adaptive neural-fuzzy inference system (ANFIS) is designed, which generates results more accurately compared to other schemes using only fuzzy system or neural network [11–14].

Moreover, the ANFIS offers more computing advantages by eliminating the construction of mathematical models, thereby decreasing the computational time needed and maintaining consistent performance in the presence of perturbations [10]. The ANFIS approach is implemented in this paper to improve the performance of a single-phase active PFC rectifier; hence, it ensures a controlled dc-link voltage regardless of the dynamic parameter changes such as load and reference output voltage. Moreover, the ANFIS controller generates the peak value of the reference current for the inner current loop. Predictive current control is a good candidate for choosing an efficient input control scheme because it offers high speed, better robustness, and low implementation complexity. There is a lot of literature focusing on predictive current control [4,8,15]. This paper uses the predictive current control to wave the shaping of the input current and improve the power factor.

In this paper, design, simulation, and real-time implementation of single-phase power factor correction based on dc bus voltage loop ANFIS controller and predictive current controller have been performed. The predictive ANFIS control strategy for the single-phase PFC

[1]Technology Faculty, Electrical Engineering Department, Automation Laboratory of Setif, University of Setif 1, Algeria
[2]LGEPC Laboratory, National Polytechnic School of Constantine, Constantine, Algeria
[3]Research Center in Industrial Technologies CRTI, Algiers, Algeria
[4]LPMRN Laboratory, Faculty of Sciences and Technology, University of Bordj Bou Arreridj, Algeria
Emails: samia.khamliche@univ-setif.dz, amar.bouafassa@enp-constantine.dz, b.babes@crti.dz, oualid.aissa@univ-bba.dz

DOI: 10.59277/RRST-EE.2024.69.2.4

is tested in MATLAB/Simulink and confirmed in real-time based on the dSPACE DS1104 control board. The simulation and experimental results have responded to the requirements of PQ and follow-up of references over a wide range of load and output voltage variations, which allows for the realization of a high-power factor for the power grid and low THD of the input current. The prominent merits of the proposed control method are:

- The less complicated architecture of the proposed control strategy;
- Fast responses;
- High dynamic performance and robustness under the step type variations in the output voltage and in the load;
- Small fluctuation and low overshoots for different operating conditions.

## 2. MODELING OF PFC BOOST CONVERTER

The dc-dc boost converter is employed to achieve the best system operations irrespective of load changes with minimum cost and high efficiency.

The basic structure of the APFC pre-regulator is illustrated in Fig. 1.

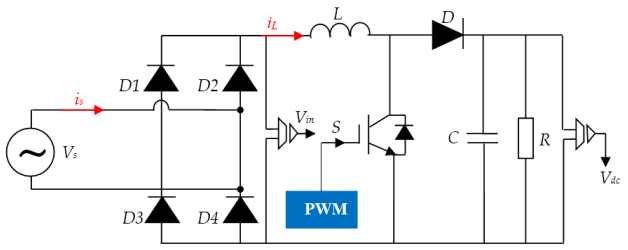


Fig. 1 – A-PFC boost converter structure.

Taking into consideration the two operation modes, the state space average model of the PFC converter is given by the following equation [6]:

$$\begin{cases} C\dfrac{dV_{dc}}{dt}=(1-S)i_L-\dfrac{V_{dc}}{R}, \\ L\dfrac{di_L}{dt}=V_{in}-(1-S)V_{dc}, \end{cases} \quad (1)$$

where $V_{in}$ and $V_{dc}$ are the input and output voltages of the circuit, respectively; $i_L$ is the input inductance current, and S is the switching state.

To get a sinusoidal input current ($i_s$) in phase with the supply voltage ($V_s$), the control unit should act so that the input voltage sees a resistive load equal to the ratio of $V_{in}$ and $i_L$ [8].

## 3. PROPOSED CONTROL APPROACHES

The active PFC boost converter's control system strategy is designed to control the dc-link output voltage and input current. Figure 2 describes the studied system with the proposed control algorithms. The system under study experiences several control challenges because of dc-link voltage and load uncertainties.

If the controller unit does not carefully control the unexpected load, it can cause instability and power quality issues. Indeed, the system comprises two control loops: the ANFIS-based dc-link voltage and predictive current controllers.

The first controller is applied to control the output voltage of the boost converter, whose inputs are: *i*) the error (e) between the measured output voltage and its reference ($e = V_{dc} - V_{ref}$) and *ii*) the error change (de), whereas its output is the peak value of reference current. The second controller is predictive control, which uses wave shaping to shape input current and improve the power quality of the circuit.

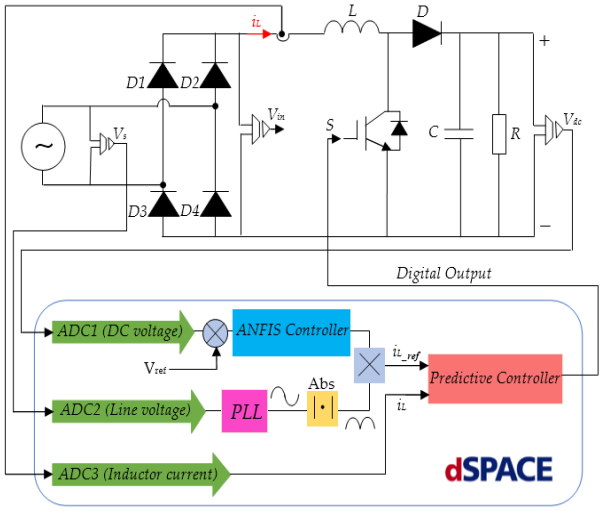


Fig. 2 – Schematic diagram of APFC converter with control loops.

### 3.1. ANFIS-BASED DC-LINK VOLTAGE CONTROLLER

Jang developed the adaptive neuro-fuzzy inference system (ANFIS) [16]. The ANFIS technique is considered a hybrid method based on the structure of ANN, and FLC deals with uncertainty efficiently. ANFIS aims to apply a hybrid learning algorithm, adopt input-output data sets, and accomplish the desired input-output mapping. The typical architecture of ANFIS of the Sugeno fuzzy system is shown in Figure 3. The ANFIS has two inputs: the voltage error (e) and its variation (de), and the single output, which is the peak value of the reference current. The if-then rules of the Sugeno fuzzy system are given as follows [10]:

$$\text{Rule 1: if e is } A_1 \text{ and de is } B_1, \text{then } u_1 = p_1 e + q_1 de + r_1$$
$$\text{Rule 2: if e is } A_2 \text{ and de is } B_2, \text{then } u_2 = p_2 e + q_2 de + r_2$$

where (e) and (de) are the inputs to ANFIS; $A_i$ and $B_i$ are the antecedent membership functions; $u_i$ is the output; $p_i$ and $q_i$ represent the weighting factors for $i^{th}$ input, and $r_i$ is the $i^{th}$ output bias.

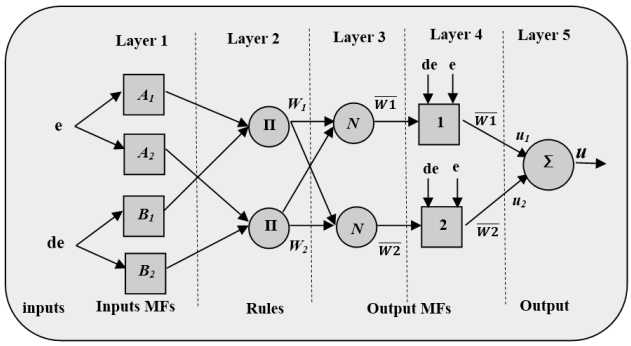


Fig. 3 – Typical five layers of ANFIS.

From Fig. 3, the ANFIS consists of five layers; the main goal of each layer is given as follows:

Layer 1 (fuzzification): neurons in this layer perform fuzzification of crisp inputs. Each node in this layer is an adaptive node where the number of these nodes equals the number of variables. This layer can be modeled by the following equation:

$$O_i^1 = \mu_{A1}(e) = \frac{1}{1+\left(\left((E-c_1)/a_1\right)^2\right)^{b_1}}, \quad (2)$$

where e is the input signal; a, b, and c are the parameters used to adjust the MFs.

Layer 2 (rule): every node in this layer is a fixed node labeled as π, which represents the premise of a rule. The output of this layer is a product of the incoming signals by the T-norm product operator as follows:

$$O_i^2 = w_i = \mu_{A1}(e) \times \mu_{B1}(de), \quad (3)$$

where $w_i$ is the firing strength of rule *i*; e and de are the input error and its change variables, respectively.

Layer 3 (normalization): this layer normalizes the firing strength of each rule according to the following equation:

$$O_i^3 = \overline{w}_i = \frac{w_i}{w_1+w_2} \quad (i = 1,2). \quad (4)$$

Layer 4 (defuzzification) is the defuzzification layer where each node in this layer is an adaptive node. The defuzzification neuron calculates the weighted consequent value by the following relation:

$$O_i^4 = \overline{w}_i \times u_i = \overline{w}_i \times (p_1 E + q_1 DE + r_1), \quad (5)$$

where $p_i$, $q_i$, and $r_i$ are the consequent parameters.

Layer 5 (output): it is the output layer; it computes the overall output value, which is linear in consequent parameters by summing all the incoming signals as per:

$$O_i^5 = u = \sum_i \overline{w}_i \times u_i \quad (6)$$

Input variables characterizing the ANFIS controller are the error e and the error variation de, and its output is the peak value of the reference current. The back-propagation learning algorithm is employed for ANFIS training. The whole process of ANFIS involves four steps: *i*) loading the training data from the model that needs to be learned; *ii*) converting the training data into a fuzzy set by designating suitable MFs and creating the "IF-THEN" rules; *iii*) updating the parameters based on the training algorithm; *iv*) converting the fuzzy values to numerical values and saves the given model. The FLC has been employed to train the proposed ANFIS scheme, which is implemented on the dSPACE 1104 control board. After that, the inputs and output values are used to train the ANFIS controller. The used FLC has two inputs (the voltage error and its variation) and a single output (the peak value of the reference current). Figure 4 shows the inputs and output MFs of the proposed ANFIS controller. Seven linguistic variables are created for implementing the ANFIS controller, such as negative big (NB), negative mean (NM), negative small (NS), zero (Z), positive small (PS), positive mean (PM), and positive big (PB). The rules of the developed ANFIS controller are tabulated in Table 1.

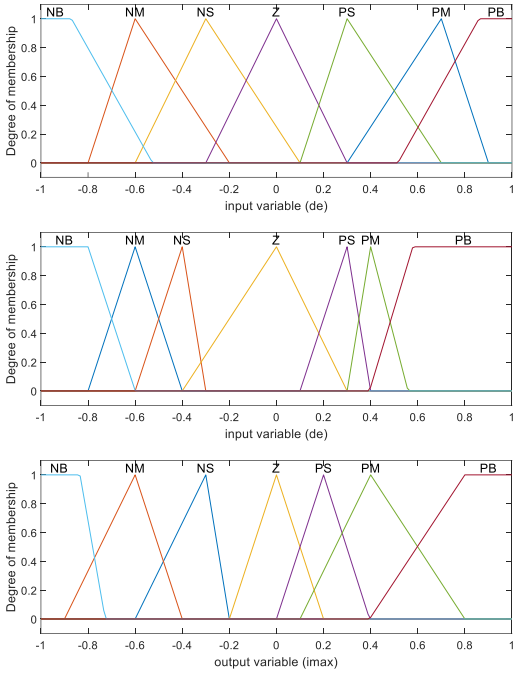


Fig. 4 – Inputs and output variables defined in the ANFIS controller.

*Table 1*

Control rule table of ANFIS used in the PFC system

| | | de(k) | | | | | | |
|---|---|---|---|---|---|---|---|---|
| $I_{max}$(k) | | NB | NM | NS | Z | PS | PM | PB |
| | NB | NB | NB | NB | NB | NM | NB | Z |
| | NM | NB | NB | NB | NM | NS | Z | PS |
| | NS | NB | NB | NM | NS | Z | PS | PM |
| | Z | NB | NB | NS | Z | PS | PM | PB |
| | PS | NM | NB | Z | PS | PM | PB | PB |
| e(k) | PM | NS | Z | PS | PM | PB | PB | PB |
| | PB | Z | PS | PM | PB | PB | PB | PB |

## 3.2 INNER CURRENT CONTROL LOOP

Among several techniques proposed for inductor current control, the predictive technique is one of the most significant candidates that have given extremely promising results during laboratory testing. Predictive current control is an interesting alternative due to its simplicity, good dynamic behavior, and flexibility. Moreover, the predictive current control (PCC) allows controlling several different system variables considering nonlinearities and constraints, greatly reducing the controller complexity [17]. This paper implements the PCC to ensure a high power factor and reduced THD by controlling the input current regardless of the changes in the treated system parameters. The PFC boost circuit has two configurations, one when the switch is ON and the other when it is OFF, as shown in Fig. 5.

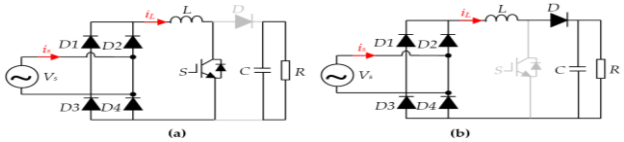


Fig. 5 – Operation modes of PFC Boost converter: a) when the switch is ON; b) when the switch is OFF.

Taking into account the switch states, the inductor current $i_L(t)$ when the switch S is turned ON or turned OFF can be written as:

- S turned ON:

$$L\frac{di_L}{dt} = v_{in}(t); \qquad t(k) \le t \le t(k) + d(k)T_s. \quad (7)$$

- S turned OFF:

$$L\frac{di_L}{dt} = v_{in}(t) - v_{dc}(t); t(k) + d(k)T_s \le t \le t(k+1). \quad (8)$$

The inductor current $i_L(t)$ for one switching cycle is depicted in Fig. 5.

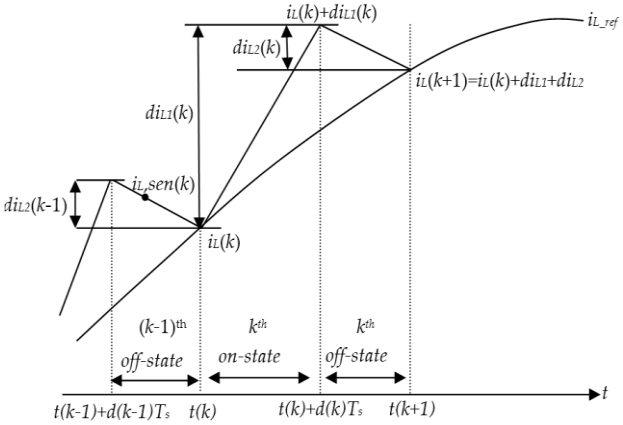


Fig. 6 – Inductor current waveform in one period.

From Fig. 6, the inductor current can be expressed as:

At: $t(k) + d(k)T_s$

$$i_L(t(k) + d(k)T_s) = i_L(t(k)) + \frac{1}{L}v_{in}(t(k))d(k)T_s. \quad (9)$$

At: $(k+1)^{th}$

$$i_L(t(k+1)) = i_L(t(k) + d(k)T_s) + \frac{1}{L}\left(v_{in}(t(k)) - v_{dc}(t(k))(1 - d(k))\right)T_s. \quad (10)$$

From Eqs. (9) and (10), the discrete form of inductor current can be written as:

$$i_L(k+1) = i_L(k) + \frac{T_s}{L}\left(v_{in}(k) - v_{dc}(k)(1 - d(k))\right). \quad (11)$$

From eq. (11), the duty cycle can be expressed as:

$$d(k) = \frac{L}{T_s}\frac{i_L(k+1) - i_L(k)}{v_{dc}} + \frac{v_{in}(k) - v_0(k)}{v_{dc}}. \quad (12)$$

Substituting $V_{dc}(k)$ and $i_L(k+1)$ in eq. (12) by its references, the duty cycle can be expressed as:

$$d(k) = \frac{L}{T_s}\frac{i_{L\_ref}(k+1) - i_L(k)}{v_{ref}} + \frac{v_{in}(k) - v_{ref}(k)}{v_{ref}}, \quad (13)$$

where the predicted reference current $i_{L\_ref}(k+1)$ is calculated as per:

$$i_{L\_ref}(k+1) = I_{max}|\sin(\omega_{Line}t(k+1)|, \quad (14)$$

where $I_{max}$ represents the peak value of the reference current that is given by the ANFIS voltage loop controller.

## 4. SIMULATION RESULTS

The results presented in Fig. 7–10 reveal the performances of ac-dc PFC boost converter based on the proposed control method at constant load conditions (R =100 Ω) with a fixed output voltage $V_{ref}$ = 180 V. Thanks to the proposed control, the following remarks are deduced from the obtained simulation results:

– Perfect input current shaping, as illustrated in Fig. 7.
– The output voltage ($V_{dc}$) remains stable at its desired value (180 V) without steady-state error and with a fast response time of < 100 ms, as illustrated in Fig. 8.
– Perfect inductor current ($i_L$) tracking as in Fig. 9.
– Unity power factor as illustrated in Fig. 10.

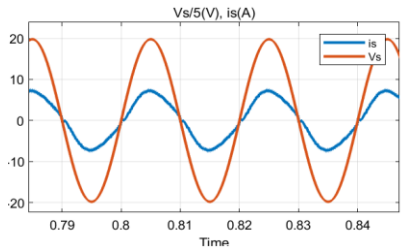


Fig. 7 – Simulation results of input voltage ($V_s$/5) and input current ($i_s$).

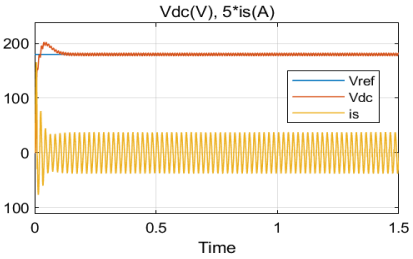


Fig. 8 – Simulation results of output voltage and input current ($5i_s$).

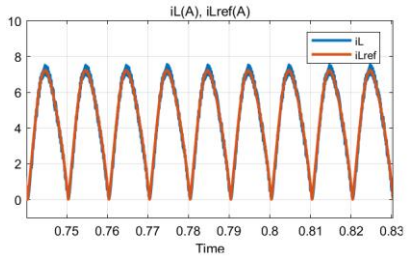


Fig. 9 – Simulation results of inductor current and reference current.

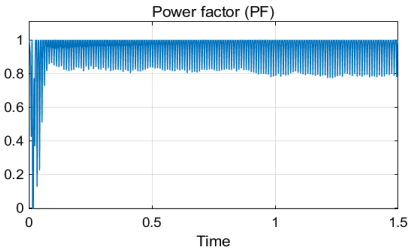


Fig. 10 – Measured PF at AC grid.

To examine the applied control performance during a transient mode, i) the reference output voltage is increased from 180 V to 220 V, and vice versa with a fixed load resistor at 100 Ω (Fig. 11). Considering Fig. 11, the robustness of the proposed control method is confirmed by the fact that the output voltage (Vdc) tracks its reference perfectly with a fast response time (less than 100 ms) and low overshoot. Also, the input current remains purely sinusoidal and unaffected

under output voltage variations, leading to a unity PF. *ii*) a 50 % step decrease and 50 % step increase in the load is applied at time instant $t$ = 0.5 s and $t$ = 1 s, respectively, with a fixed output voltage of 180 V (Fig. 12). From Fig. 12, the output voltage ($V_{dc}$) remains stable at desired value with a small fluctuation.

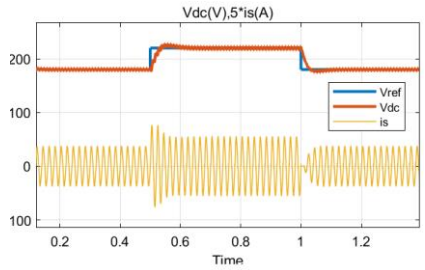


Fig. 11– Simulation results of reference output voltage variations from $V_{dc}$ = 180 V to $V_{dc}$ = 220 V, and inversely.

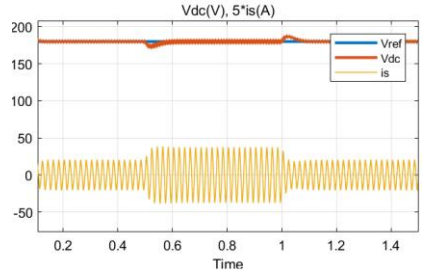


Fig. 12– Transient of the step-change of the load from 100 Ω to 50 Ω and inversely.

## 5. EXPERIMENTAL VERIFICATIONS

A purpose-built experimental setup, illustrated in Figure 13, was commissioned to implement the proposed control technique for the PFC converter using a dSPACE DS1104 control board.

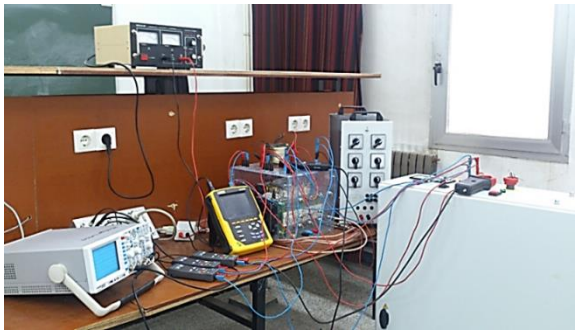

Fig. 13 – Experimental test bench.

### 5.1. STEADY-STATE WAVEFORMS

The experimental steady-state waveforms under constant load and output voltage are depicted in Figs. 14–15. The steady-state behavior is very satisfying where the input current ($i_s$) is in sinusoidal waveform (Fig. 14a) with low THD at ac mains (3.5 %) (Fig. 14b), that complies with the IEEE-519 standard (THD ≤ 5 %) [3], and the PF is about 0.990 (Fig. 15a), which enhances the energy efficiency via unity PF operation. On the other hand, it can be observed that the measured inductor current has the same form of its reference as indicated in Fig. 15b.

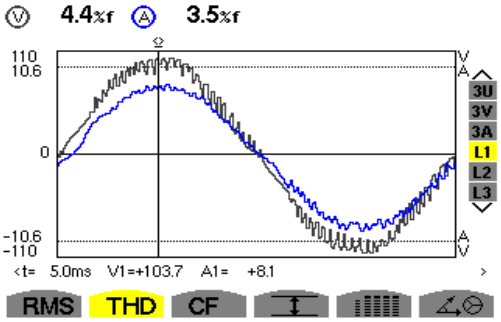


(a)

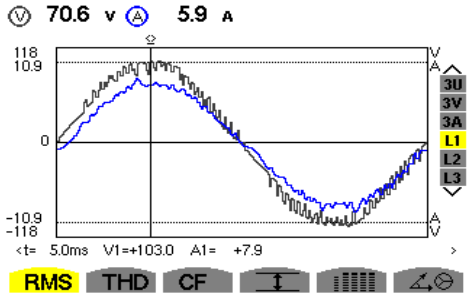


(b)

Fig. 14 – Experimental results of: a) supply voltage ($V_s$) and current ($i_s$); b) THD.

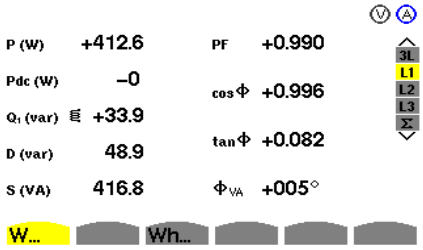


(a)

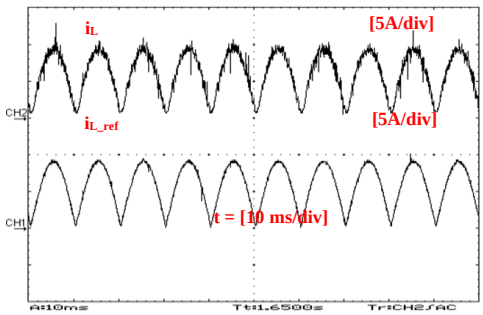


(b)

Fig. 15 – Measured results of: a) power factor (PF); b) inductor current ($i_L$) (CH1) and its reference ($i_{L\_ref}$) (CH2) (5 A/div).

### 5.2. EXPERIMENTAL RESULTS UNDER OUTPUT VOLTAGE VARIATIONS

During this experiment, the reference output voltage steps from 180 V (100 %) to 250 V (139 %) and from 250 V to 180 V, respectively. The results for the controlled output voltage ($V_{dc}$) and the input current ($i_s$) are shown in Figure 16. It can be seen from this figure that the controlled output voltage tracks their desired value ($V_{ref}$) in a very satisfying manner without noticeable overshoot. The dc-link voltage reached its new reference (250 V) after 0.195 s and needed 0.180 s to return to 180 V. Moreover, the input current is presented by its sinusoidal form, which leads to the functioning of our system under unitary PF.

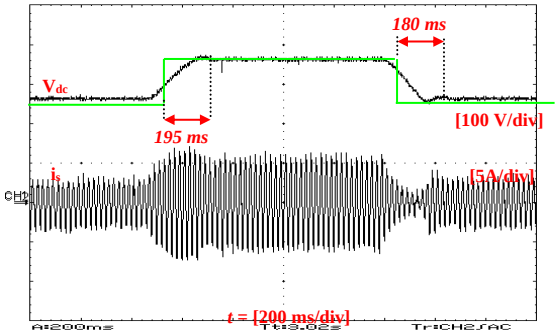


Fig. 16 – Output voltage variations.

### 5.3. EXPERIMENTAL RESULTS UNDER LOAD VARIATIONS

The proposed control strategy should also be robust enough to handle this disturbance. Hence, the load varies during this experiment while the output voltage remains constant ($V_{dc}$ = 180 V). The load decreased from 100 Ω (full load) to 50 Ω (part load) and back to 100 Ω, as shown in Fig. 17. The obtained experimental result displays an almost sinusoidal input current ($i_s$) waveform and a constant output voltage ($V_{dc}$), very close to its reference value ($V_{ref}$) with the presence of a slight transient drop and rise of 0.2 s.

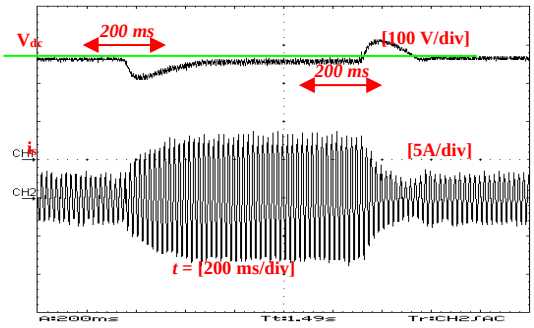


Fig. 17–Experimental results of output voltage ($V_{dc}$) transient responses during a load change, from R = 100 Ω to R = 50 Ω and inversely.

## 6. **CONCLUSIONS**

This paper has described a novel control scheme to improve the power factor of AC/DC boost rectifiers based on adaptive neural-fuzzy inference and predictive current controller, where simulation and real-time implementation studies are presented. Various experiments and tests have been performed in different working conditions. Sudden load changes and reference output voltage variation were considered typical industrial requirements. The validity and efficiency of the proposed methodology have been proved through simulations and experiments. Obtained practical results are as follows:

- A steady-state analysis has shown that the power factor has reached 0.990, and the THD of the input current is less than 5 %, which complies with the IEEE-519 standard.
- A transient state analysis has shown that the output voltage is unaffected during out-put load variations while neglecting steady-state error.
- The time required to reach the desired value during variations in output voltage is very small. Indeed, to increase the measured output voltage to its reference, 200 ms is sufficient to achieve this objective.

*Received on 3 July 2023*

## REFERENCES

1. B. Singh, B.N. Singh, A. Chandra, K. Al-Haddad, A. Pandey, D.P. Kothari, *A review of single-phase improved power quality ac-dc converters*, IEEE Trans. Ind. Electron., **50**, pp. 962–981 (2003).
2. A. Karaarslan, A. Iskender, *DSP based power factor correction converter to reduce total harmonic distortion of input current for improvement of power quality*, Electr. Eng., **93**, pp. 247–257 (2011).
3. R.C. Dugan, M.F. McGranaghan, S. Santoso, H. Wayne Beaty, *Electrical power system quality*, 2nd edition, McGraw-Hill, 2003.
4. A. Bouafassa, L. Rahmani, S. Mekhilef, *Design and real-time implementation of single-phase boost power factor correction converter*, ISA Trans., **55**, 267–274 (2015).
5. K. Kayisli, S. Tuncer, M. Poyraz, *A novel power factor correction system based on sliding mode fuzzy control*, Electric power components and systems, **45**, 430–441 (2017).
6. A. Kessal, L. Rahmani, *GA-optimized parameters of sliding-mode controller based on both output voltage and input current with an application in the PFC of ac/dc converters*. IEEE Trans. Power Electron., **29**, 3159–3165 (2014).
7. J.D. Faucher, S. Caux, P. Maussion, *Fuzzy controller tuning of a boost rectifier unity power factor correction by experimental designs*, Electr. Eng, **91**, 167–176 (2009).
8. A. Bouafassa, L. Rahmani, A. Kessal, B. Babes, *Unity power factor converter based on a fuzzy controller and predictive input current*. ISA Trans., **53**, 1817–1821 (2014).
9. C. Komathi, M.G. Umamaheswari, *Design of gray wolf optimizer algorithm-based fractional order pi controller for power factor correction in SMPS applications*. IEEE Trans. Power Electron., **35**, pp. 2100–2118 (2020).
10. A. Benyamina, S. Moulahoum, I. Colak, R. Bayindir, *Design and real-time implementation of adaptive neural-fuzzy inference system controller based unity single phase power factor converter*. Electr. Power Syst. Research, **152**, pp. 357–366 (2017).
11. N. Priyadarshi, S. Padmanaban, J.B. Holm-Nielsen, F. Blaabjerg, M.S. Bhaskar, *An experimental estimation of hybrid ANFIS–PSO-based MPPT for PV grid integration under fluctuating sun irradiance*. IEEE syst. Journal, **14**, pp. 1218–1229 (2020).
12. D. Mlakić, H.R. Baghaee, S. Nikolovski, *A novel ANFIS-based islanding detection for inverter-interfaced microgrids*. IEEE Trans. Smart Grid, **99**, pp. 1–13 (2018).
13. L. Senthil Murugan, P. Maruthupandi, *Sensorless Speed control of 6/4-pole switched reluctance motor with ANFIS and fuzzy-PID-based hybrid observer*, Electr. Eng., **102**, pp. 831–844 (2020).
14. A. Alice Hepzibah, K. Premkumar, *ANFIS current–voltage controlled MPPT algorithm for solar powered brushless dc motor-based water pump*, Electr. Eng., **102**, pp. 421–435 (2020).
15. A. Bouafassa, L. Rahmani, B. Babes, R. Bayindir, *Experimental design of a finite state model predictive control for improving power factor of boost rectifier*, Proceedings of the IEEE 15th International Conference on Environment and Electrical Engineering (EEEIC), pp. 1556–1561 (2015).
16. J.S. Jang, *ANFIS adaptive-network-based fuzzy inference system*, IEEE Trans. Syst. Man Cybern., **23**, pp. 665–685(1993).
17. L.N. Ramya, A. Sivaprakasam, *Application of model predictive control for reduced torque ripple in orthopedic drilling using permanent magnet synchronous motor drive*, Electr. Eng., **02**, *3*, pp. 1469–1482 (2020).